J Nanostruct 15(4): 2438-2446, Autumn 2025

RESEARCH PAPER

Studying the Structural, Electrical Properties and Antibacterial Applications of PMMA-PEO/SiO_2 Nanocomposites

Hussein Ali Hadi *, ***Sameer H. Al-nesrawy, Shurooq S. Al-Abbas***

Department of Physics. College of Education for Pure Sciences, University of Babylon. Babylon, Iraq

ARTICLE INFO

Article History:
Received 05 May 2025
Accepted 24 September 2025
Published 01 October 2025

Keywords:
Antibacterial
Electrical properties
Nanocomposite
Structural properties
PMMA-PEO/SiO_2

ABSTRACT

This study focuses on the production of PMMA-PEO/SiO_2 nanocomposites by adding varying amounts of silicon oxide (0, 1.4, 2.8, 4.2, and 5.6%). This research addresses the incorporation of SiO_2 nanoparticles into PMMA-PEO polymer blends. The electrical and structural properties of the PMMA-PEO matrix were studied by adding nanoparticles at varying ratios. FTIR investigations revealed the functional groups and chemical bonds of the nanocomposites. The structural, electrical, and FTIR properties of the nanocomposites were proposed. FESEM examinations demonstrated the surface structure of the nanocomposites and the homogeneous formation of silicon oxide nanomaterials with PMMA-PEO polymers. Applying an electric field increased the frequency, decreased the dielectric constant, and reduced electrical losses. The data revealed the amount of electrical loss in each sample and the extent to which the dielectric constant increased with increasing silicon oxide content. This phenomenon was observed in relation to the electrical conductivity of alternating current. In addition, PMMA-PEO/SiO_2 nanocomposites were prepared, and these composites demonstrated their ability to inhibit bacterial growth. This inhibition ability increased with increasing the number of SiO_2 nanoparticles. The results demonstrated that the laboratory-prepared nanocomposites possess unique properties, combining the electrical properties of silicon oxide with those of PMMA and PEO polymers. Samples were placed in a Mueller-Hinton medium at 34–37 °C for 24 hours for both gram-negative and gram-positive bacteria. Laboratory tests also demonstrated that these nanocomposites effectively inhibited the growth of various types of bacteria, including Staphylococcus aureus and Klebsiella pneumoniae, including antibiotic-resistant bacteria.

How to cite this article
Hadi H., Al-nesrawy S., Al-Abbas S. Studying the Structural, Electrical Properties and Antibacterial Applications of PMMA-PEO/SiO_2 Nanocomposites . J Nanostruct, 2025; 15(4):2438-2446. DOI: 10.22052/JNS.2025.04.080

INTRODUCTION

Nanocomposites demonstrate remarkable properties owing to a distinctive amalgamation of constituents. The swift demand for elastomers and engineered plastics is noteworthy [1]. Their applications span several industries, including packaging and other purposes [2,3]. Nanotechnology involves the creation and utilisation of nanocomposites, offering innovative methods and commercial prospects across multiple industries, such as automotive, aerospace, superconductors, electronics, and

---

* *Corresponding Author Email: lyh026967@gmail.com*

both physical and chemical fields, with dimensions spanning from individual molecules or atoms to submicron scales [4-7]. Nanotechnology is often seen as the next industrial revolution. Nanocomposite polymers, including organic polymers and nanoscale inorganic nanoparticles, are novel materials that have attracted significant interest in recent years [8,9]. These composite materials differ from pure polymers in both chemical and physical properties [10,11]. This might be very substantial and advantageous for several candidates across multiple applications [12,13]. The incorporation of nanoparticles into a polymer matrix may substantially improve the optical characteristics of the material with modest amounts of nanoparticles. One advantage of nanoparticles as polymer additions, compared to conventional additives, is their minimal loading needs, attributable to their substantial influence on physical characteristics [10]. The optical properties of polymers are essential for investigating electronic transitions and their prospective use as optical filters. Data on the electrical structures of amorphous and crystalline semiconductors is often acquired by analysing optical characteristics over extensive frequency ranges [4]. Polymethyl methacrylate (PMMA) is a linear thermoplastic polymer. The melting point is 160 °C, while the glass transition temperature is 115°C [14]. PMMA exhibits superiority One semicrystalline polymer with potential bio-electrochemical usage is poly(ethylene oxide) (PEO) [15-18]. At temperatures beyond its melting point, PEO's optical and electromagnetic properties

are insufficient, which is its only drawback in practical applications. In order to improve its features [19,20]. In order to achieve thermal stability beyond the nanocomposite's melting point, PEO nanocomposite structures, which include nanoparticles, have strong interactions with surface functional groups [21]. Incorporating a variety of nanocomposites put into PEO material may improve its qualities and increase its applicability in many fields [22]. The number 23. Because of its unique chemical properties, PEO has found widespread usage in a variety of contexts [23,24]. Silica (SiO_2) is also known as silicon dioxide. Among the many interesting properties of silicon

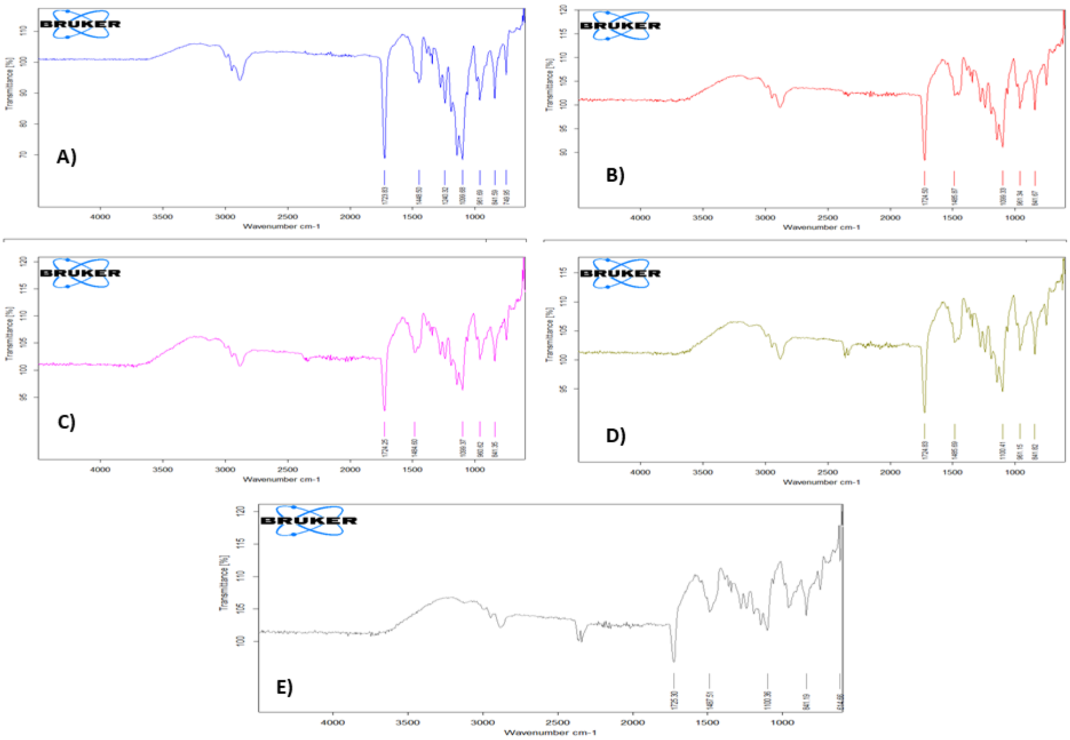

Fig. 1. FT-IR spectra (PMMA-PEO/SiO_2) Nanocomposite materials: (A) for blend, (B) 1.4 wt.%, (C) 2.8 wt.%, (D) 4.2 wt.% and (E) 5.6 wt.%.

dioxide nanoparticles (SiO_2) are their low toxicity, biocompatibility, physiologically degradability, cheap cost, and thermal and chemical stability. They may also be functionalised with a wide range of agents and plastics. Glass, steel, chemical strands, plastic, batteries, paints, makeup, and other environmental protection Businesses in may also find extensive application for nano-silica. The strength, hardness, wear, and age resistance of polymers enhanced by silica nanoparticles are much greater [25].

MATERIALS AND METHODS

The casting procedure was used to create the (PMMA-PEO/ SiO_2) nanocomposite. At room temperature, 1 gramme of (PMMA-PEO) and SiO_2 were dissolved in 50 millilitres of chloroform alcohol using a magnetic stirrer to thoroughly mix and dissolve the material. The weight ratios of SiO_2 nanoparticles added to PMMA-PEO were(1.4,2.8,4.2, and 5.6%. Using a 10-centimeter-diameter Petri dish as a mould, pouring the liquid in, waiting for it to dry, and then carefully removing it for testing is the casting procedure.

RESULTS AND DISCUSSION

FTIR spectra of (PMMA/PEO/SiO_2) nanocomposites

Fig. 1 depicts the various peaks in FT-IR spectra of (PMMA-PEO/SiO_2) nanocomposites at distinct concentrations (pure, 1.4, 2.8, 4.2, 5.6wt %) of (SiO_2), which are situated within the range of (4000 - 500) cm^{-1}. Fig. 1-a illustrates the FTIR spectrum of (PMMA-PEO/SiO_2), which features a prominent peak near (1723.83) cm^{-1}, corresponding to the carbonyl stretching (C=O), primarily indicating the interaction between PMMA and PEO. The bending vibration of (CH2) is seen at 1448.50 cm^{-1}, whereas the stretching vibration of the (C-O) group occurs at 1099.68 cm^{-1}. Fig. 1-b also exhibits several peaks, specifically at 1485.87 cm^{-1} and 1099.33 cm^{-1},

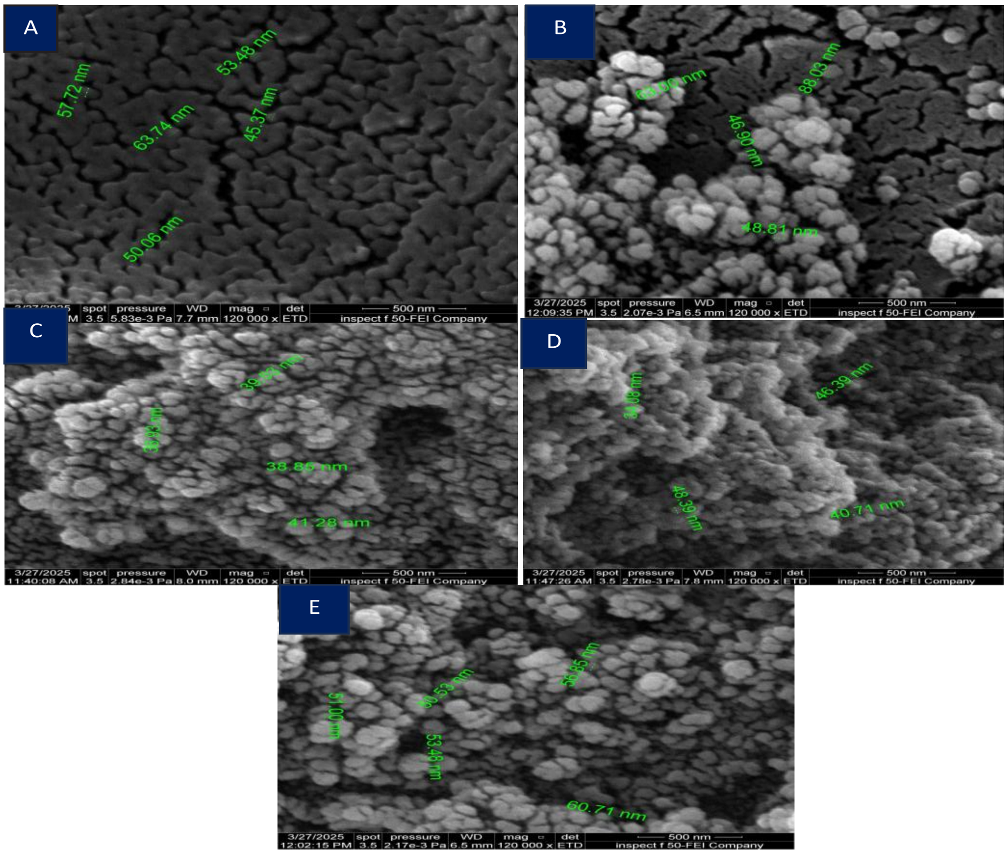

Fig. 2. The FESEM of PMMA-PEO/ SiO_2 complex materials: (a) of (PMMA-PEO), (b) of 1.4 wt.% SiO_2, (c) of 2.8wt.% SiO_2, (d) of 4.2 wt.% SiO_2 and e) of 5.6 wt.% SiO_2.

which correspond to the (CH_2) and (C-O) bonds, respectively. The signal detected at 1724.50 cm^{-1} pertains to the carbonyl (C=O) functional group. The peak at 1099.33 cm^{-1} is the (C-O) The carbonyl group being stretched of the pmma compound. This (C-H) bending occurs at a peak of 961.34 cm^{-1}, outside the absorption plane of the rings. In Fig. 1-C, peaks are discerned at 1724.25 cm^{-1} and 1099.37 cm^{-1}. The peak at 1724.25 cm^{-1} relates to the stretching vibration of the PMMA's carbonyl group polymer. In comparison, the peak at 1099.37 cm^{-1} is linked to the stretching vibration of the C-O bond, accompanied by an additional absorption peak at 960.62 cm^{-1} connected with the bending of the rings. The FT-IR is presented [26]. Fig. 1-d demonstrates that the peak at 1724.83 cm^{-1}is attributable to (C=O). Distinct peaks of (C-H) bending and (C-O) stretching are observed at 961.41 cm^{-1} and 1100.41 cm^{-1}, respectively. Fig. 1-e depicts the peaks at 1725.30 cm^{-1} associated with the (C=O) group. While at the peak 1100.36 cm^{-1}, (C-O) stretching. The FT-IR measurements demonstrate that no chemical reaction occurs; physical bonding or contacts are evident [27,28].

Field-emission scanning electron microscope (FESEM)

The arrangement of silicon oxide (SiO_2 nanoparticles) within the polymer is examined through field-emission scanning electron

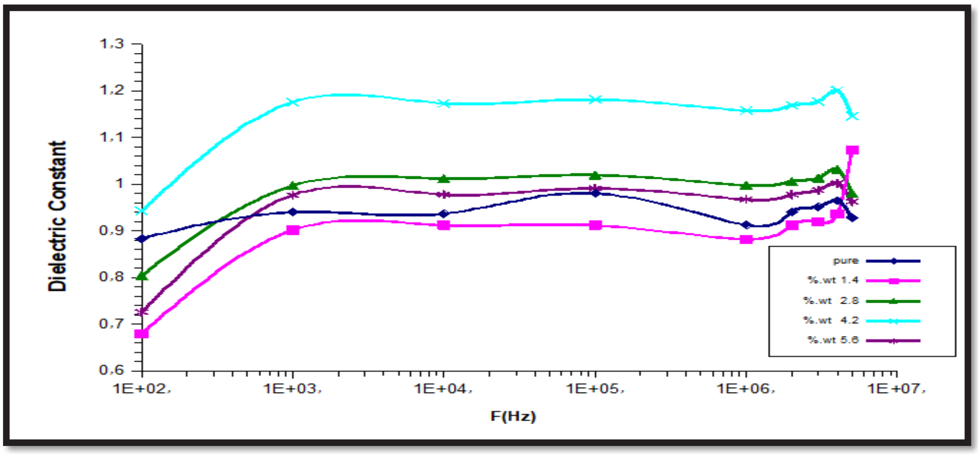

Fig. 3. Dielectric constant performance of nanocomposites as a function of frequency

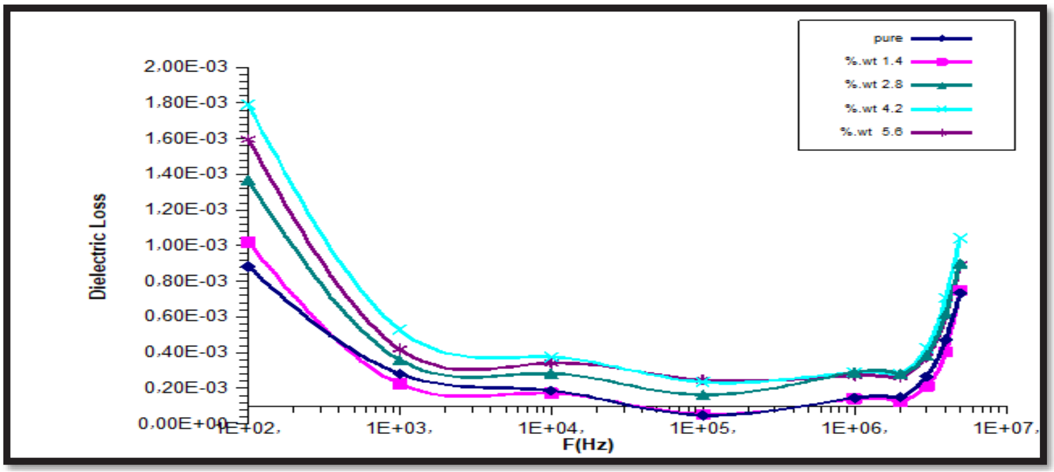

Fig. 4. Dielectric loss performance of nanocomposites as a function of frequency.

microscopy (FESEM), and the influence of these particles on the nanocomposites is assessed. Fig. 2 present FESEM images of films derived from PMMA-PEO/ SiO_2 nanocomposites, exhibiting different concentrations of Si and SiO_2 nanoparticles The.incorporation of silicon oxide (SiO_2 nanoparticles) within the polymer matrix was analysed using field-emission scanning electron microscopy (FESEM), and the effects of these particles on the properties of the nanocomposites were assessed. Fig. 2 presents FESEM images of films derived from PMMA-PEO/ SiO_2 nanocomposites, showcasing varying concentrations of SiO_2 nanoparticles. Fig. 2-a demonstrates the cohesiveness and homogeneity of the polymer, showing that the addition of SiO_2 nanoparticles to the PMMA-PEO polymer modifies the surface structure of the system, as evidenced by images B, C, D, and E in the figure. The average grain sizes derived from the FESEM images were 61.6 nm, 39.6 nm, 33.9 nm, and 54.51 nm for SiO_2 nanoparticles at concentrations of 1.4%, 2.8%, 4.2%, and 5.6%, respectively. FESEM images demonstrate a reduction in average grain size of 2.8% and 4.2% upon the incorporation of silicon dioxide nanoparticles, succeeded by an increase of 5.6%. This is consistent with the researchers' findings [29].

The Results of A.C. Electrical Properties

Dielectric constant (ε›) and dielectric loss (ε››) of (PMMA-PEO/SiO_2) Nanocomposites

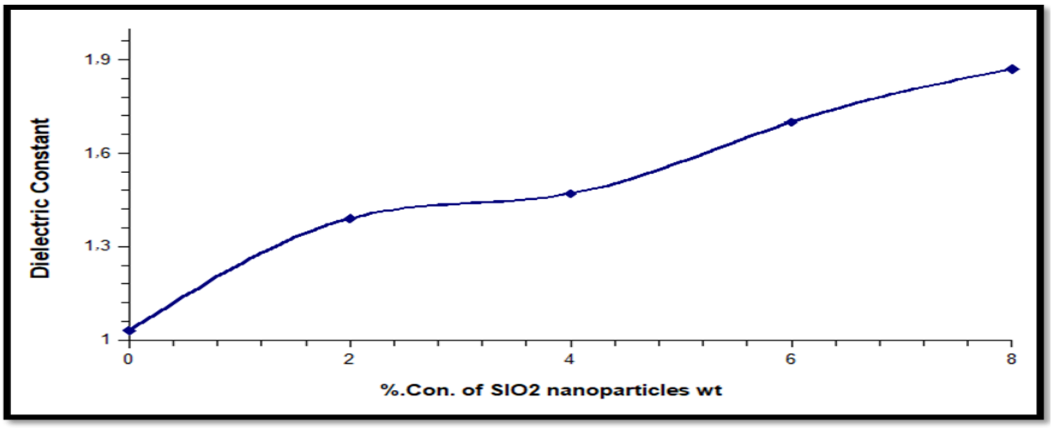

Fig. 5. Dielectric constant performance for (PMMA-PEO) blends with a concentration of nanocomposites.

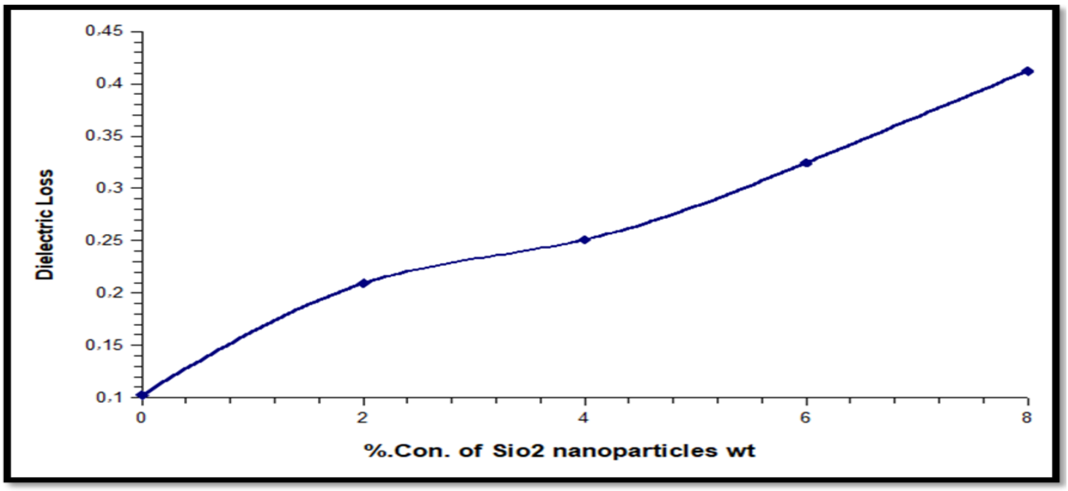

Fig. 6. Dielectric loss performance in nanocomposites with varying concentrations of (SiO_2) nanocomposites.

Figs. 3 and 4 demonstrate that the dielectric constant and dielectric loss fluctuate with frequency for nanocomposites consisting of (PMMA-PEO/SiO_2). The images illustrate that Maxwell-Wagner polarization results in elevated dielectric constants and losses at low frequencies. Nevertheless, when the frequency increases, these values decrease across all samples. The contacts between insulators and conductors produce this polarization. The buildup of dipoles or space charges at interfaces results in polarization on those surfaces. As the frequency of the electric field that is being used diminishes, the reaction time of the space charges increases. Nevertheless, the polarization effect diminishes when the electric field fluctuates rapidly within the higher frequency spectrum. The loss of dielectric and the dielectric constant diminish as the frequency increases. This behaviour supports the researchers' conclusions [30].

Figs. 5 and 6 illustrate the correlation between the dielectric constant and dielectric loss as a function of the density of (PMM-PEO/ SiO_2) nanoparticles at room temperature and (100)

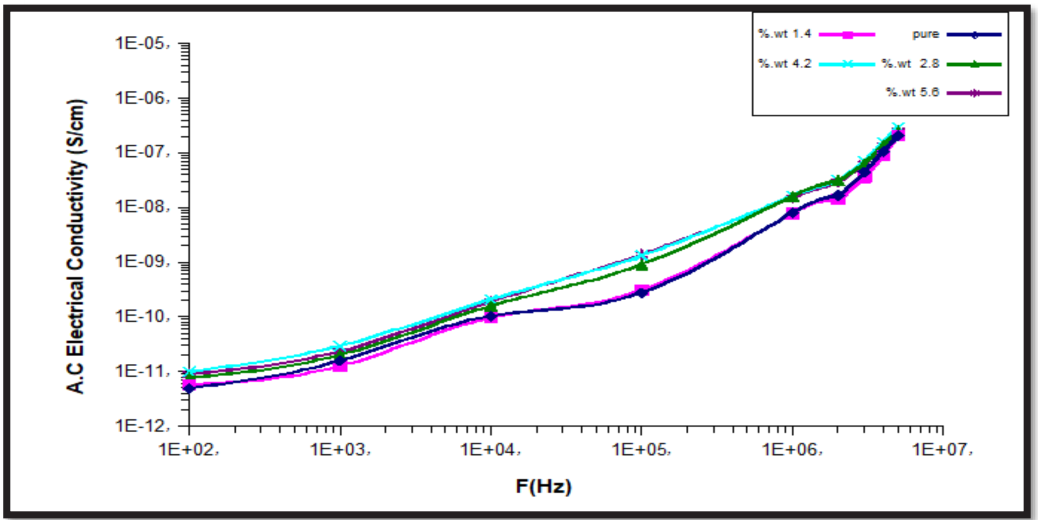

Fig. 7. The relation between A.C electrical conductivity with frequency for (PMMA-PEO/ SiO_2) nanocomposites.

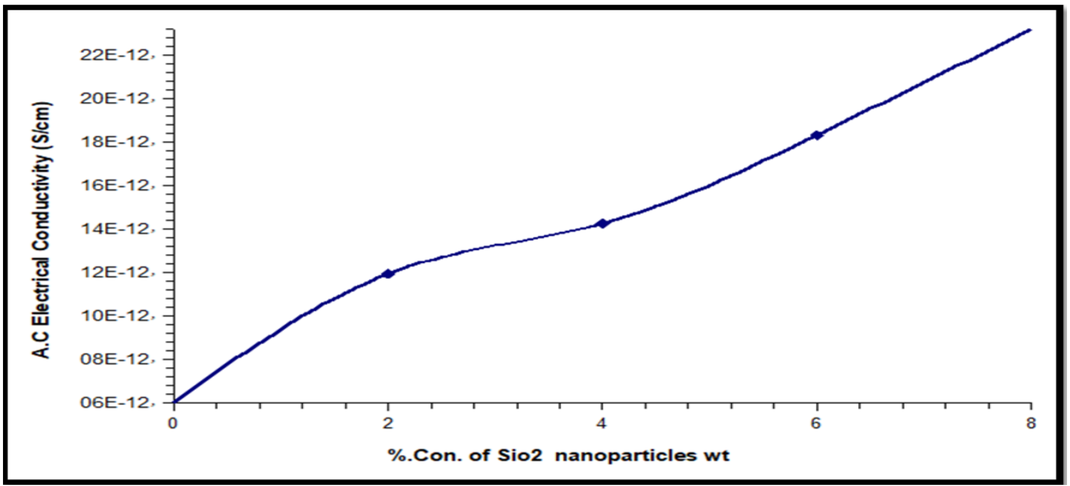

Fig. 8. Effect of (SiO_2) nanoparticle concentrations on A.C electrical conductivity of PMMA-PEO.

Hz. We determine the dielectric constant and dielectric loss of PMM-PEO/ SiO_2 using the formulae ($\varepsilon' = Cp/Co$) and ($\varepsilon'' = \varepsilon' D$). Darker and smaller regions signify a decreased concentration of (PMM-PEO/ SiO_2) nanoparticles. These patches develop at a concentration comparable to that of PMM-PEO/ SiO_2 nanoparticles. The network will have overlapping routes that interconnect some regions with many nanoparticles, facilitating the movement of charge carriers. With a rise in the density of (PMM-PEO/ SiO_2) nanoparticles, both the dielectric constant and dielectric loss elevate, ascribed to the augmented quantity of free Carriers of charge and polarization charges. This discovery aligns with [31].

Electrical conductivity of (PMMA-PEO/SiO_2) nanocomposites

The A.C. conductivity of nanocomposites is calculated by using the equation ($\sigma A.C = w\, \varepsilon_o\, \varepsilon''$) . The variation in alternating current (AC) electrical conductivity for (PMMA-PEO/ SiO_2) nanocomposites is shown in Fig. 7. This variation is demonstrated as a function of the frequency of the electric field at room temperature. As can be seen in the illustration, the electrical conductivity of alternating current increases with frequency. This is because space charge polarization causes the conductivity to increase. In order to contribute to this phenomenon, low-frequency space charge polarization and the stimulation of charge carriers to higher states in the conduction band are both elements that are involved [32]. Electronic polarization and the mobility of charge carriers are the two factors that contribute to the improvement of conductivity at higher frequencies. The velocity of the primary chain and the flow of ions are the two factors that have an effect on the conducting capacity of alternating current. At a frequency of 100 hertz, the influence of the concentration of SiO_2 nanoparticles on the conductivity of electricity of the PEO-PMMA mix is shown in Fig. 8. Because of the concentration of SiO_2 nanoparticles, there is an increase in the charge carrier density inside the polymer medium, which leads to an increase in the alternating current electrical conductivity.[33].

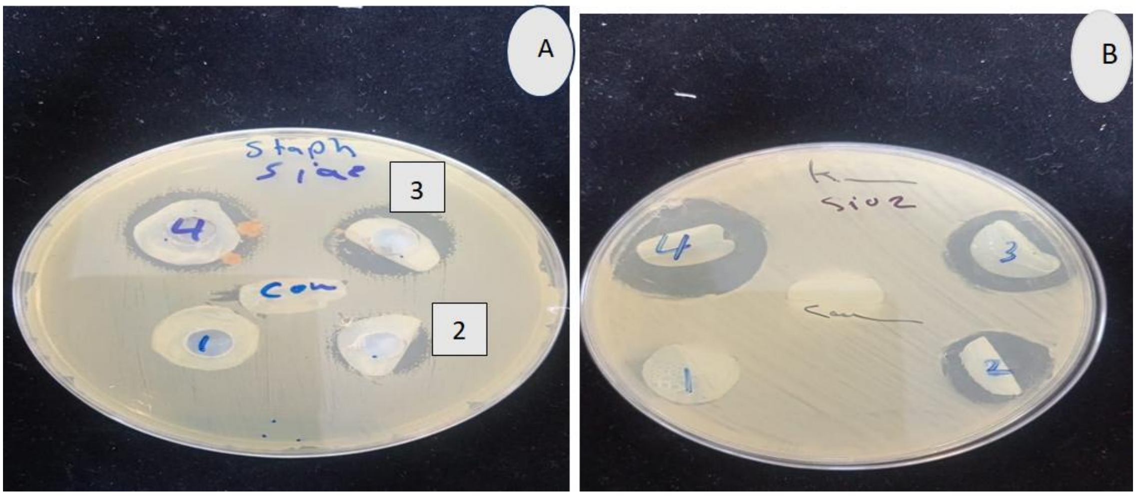

Fig. 9.)A) Images of the inhibition zone for Staphylococcus. (B) Images of the inhibition zone for Klebsiella pneumoniae.

Table 1. inhibition zone diameter of (PMMA-PEO/SiO_2) nanocomposites.

concentrations (SiO_2) wt%	Inhibitions zone diameter(mm) of Staphylococcus	Inhibitions zone diameter(mm) of Klebsiella pneumoniae
pure	0	0
1.4	14	13
2.8	17	19
4.2	19	21
5.6	22	23

Application of (PMMA-PEO/SiO_2) nanocomposites for antibacterial efficacy

A visual representation of the inhibitory zones for Staphylococcus and Klebsiella pneumoniae may be found, as shown in Fig. 9, The antibacterial effectiveness of nanocomposites composed of polymethyl methacrylate (PMMA) and polyethylene oxide (SiO_2) was assessed for both gram-positive bacteria (Staphylococcus aureus) and gram-negative microbes (Klebsiella pneumoniae). Based on the findings, it can be seen that the diameter of the inhibitory zone augmentations as the density of SiO_2 Nanoparticles increases [34]. It is increased from 0 mm to 23 mm for the Klebsiella pneumoniae and from 0 mm to 22 mm for the S. aureus for the PMMA - PEO / SiO_2 It is possible that the antimicrobial agent effectiveness of the nanocomposites might be attributed to the production of reactive oxygen species (ROS) by a variety of nanoparticle molecules. There is a possibility that the oxidative stress brought about by reactive oxygen species (ROS) is the fundamental mechanism that is responsible for the antibacterial activity of nanocomposites that are formed by nanoparticles. There are a number of radicals that are included in reactive oxygen species (ROS). These radicals include There are four types of radicals: superoxide (O_2), hydroxyl (-OH), hydrogen peroxide (H_2O_2), and singlet oxygen (-O_2).

In bacteria, it has the potential to cause damage to both DNA and proteins. Possibly, the generation of reactive oxygen species by silicon dioxide was responsible for the suppression of the most hazardous microbes. On the other hand, the nanoparticles that are included inside the nanocomposites have negative charges, which causes an electromagnetic attraction to exist between them and the microbes contained within them. After the attraction has been formed, the microorganisms will go through the process of oxidation and will eventually die [35]. With regard to the nanocomposites composed of PMMA-PEO/ SiO_2, the width of the inhibitory zone is shown in Table 1.

CONCLUSION

FTIR analysis revealed no chemical interaction between the SiO_2 nanoparticles and the polymers used in the PMMA-PEO/ SiO_2 nanocomposites. FESEM examination revealed the homogeneity of the silicon dioxide and PMMA-PEO nanocomposites, and that the average grain size decreased with increasing SiO_2 content. The study revealed a decrease in the dielectric constant ε' of the samples with increasing applied electric field strength, a trend consistent with the observed dielectric loss patterns ε''. Increasing frequency enhanced the alternating current electrical conductivity of the PMMA-PEO/ SiO_2 nanocomposites. The dielectric loss and dielectric constant values increased at all concentration combinations with increasing silicon dioxide content. The antibacterial activity of the PMMA-PEO/ SiO_2 nanocomposites indicated that the zone of inhibition against Staphylococcus aureus and Klebsiella pneumoniae increased with increasing amounts of silicon dioxide nanoparticles. This demonstrates the potential of nanomaterials in medical applications, such as killing and inhibiting bacteria, and electrical and industrial applications.

CONFLICT OF INTEREST

The authors declare that there is no conflict of interests regarding the publication of this manuscript.

REFERENCE

1. Paul DR, Robeson LM. Polymer nanotechnology: Nanocomposites. Polymer. 2008;49(15):3187-3204.
2. Papirer E. The effect of filler shape on the mechanical properties of a reinforced vulcanizate: The SBR-ground asbestos system. Journal of Polymer Science: Polymer Chemistry Edition. 1983;21(9):2833-2836.
3. Moniruzzaman M, Winey KI. Polymer Nanocomposites Containing Carbon Nanotubes. Macromolecules. 2006;39(16):5194-5205.
4. Kadhim MA, Al-Bermany E. Structural and DC-electrical properties of novel PMMA-PVA nanocomposites reinforced with graphene nanosheets. IOP Conference Series: Materials Science and Engineering. 2021;1067(1):012120.
5. Abdulridha AR, Al-Bermany E, Hashim FS, Omran Alkhayatt AH. Synthesis and characterization and pelletization pressure effect on the properties of $Bi_{1.7}Pb_{0.3}Sr_2W_{0.2}Ca_2Cu_3\ O_{10+\delta}$ superconductor system. Intermetallics. 2020;127:106967.
6. Mohamed Ali T, Padmanathan N, Selladurai S. Effect of nanofiller CeO2 on structural, conductivity, and dielectric behaviors of plasticized blend nanocomposite polymer electrolyte. Ionics. 2014;21(3):829-840.
7. Al-Bermany E, Qais D, Al-Rubaye S. Graphene Effect on the Mechanical Properties of Poly (Ethylene Oxide)/ Graphene Oxide Nanocomposites Using Ultrasound Technique. Journal of Physics: Conference Series. 2019;1234(1):012011.
8. Abdelamir AI, Al-Bermany E, Hashim FS. Important factors affecting the microstructure and mechanical properties of PEG/GO-based nanographene composites fabricated applying assembly-acoustic method. AIP Conference Proceedings: AIP Publishing; 2020. p. 020110.
9. Vaia RA, Maguire JF. Polymer Nanocomposites with

Prescribed Morphology: Going beyond Nanoparticle-Filled Polymers. Chem Mater. 2007;19(11):2736-2751.

10. Haque SR, Boro P, Phukan P, Bhattacharjee S. A comparative study between PANI, PANI/PbS and PANI/PbS/ZnO core/shell quantum dots as chemiresistive sensor for the detection of formaldehyde gas. Journal of Materials Science: Materials in Electronics. 2024;35(30).
11. Kinetic and thermodynamic study of adsorption of an industrial food dye using Iraqi clay. Journal of Population Therapeutics and Clinical Pharmacology. 2023;30(5).
12. Cabassi R, Delmonte D, Abbas MM, Abdulridha AR, Gilioli E. The Role of Chemical Substitutions on Bi-2212 Superconductors. Crystals. 2020;10(6):462.
13. Oboudi SF, Al-Habeeb MQ. Gold Nanoparticles Effect on (Bi,Pb)-2223 Superconducting Thin Films. Applied Physics Research. 2016;8(5):64.
14. Abdelrazek EM, Hezma AM, El-khodary A, Elzayat AM. Spectroscopic studies and thermal properties of PCL/PMMA biopolymer blend. Egyptian Journal of Basic and Applied Sciences. 2016;3(1):10-15.
15. Thakur VK, Vennerberg D, Madbouly SA, Kessler MR. Bio-inspired green surface functionalization of PMMA for multifunctional capacitors. RSC Advances. 2014;4(13):6677.
16. Alsaad AM, Ahmad AA, Qattan IA, El-Ali A-R, Fawares SAA, Al-Bataineh QM. Synthesis of Optically Tunable and Thermally Stable PMMA–PVA/CuO NPs Hybrid Nanocomposite Thin Films. Polymers. 2021;13(11):1715.
17. Yang XQ, Lee HS, Hanson L, McBreen J, Okamoto Y. Development of a new plasticizer for poly(ethylene oxide)-based polymer electrolyte and the investigation of their ion-pair dissociation effect. J Power Sources. 1995;54(2):198-204.
18. Miscibility, Thermal Properties and Ion Conductivity of Poly(Ethylene Oxide) and Polyacrylate. Physical Chemistry of Macromolecules: Apple Academic Press; 2014. p. 519-588. http://dx.doi.org/10.1201/b16706-25
19. Ratna D, Divekar S, Samui AB, Chakraborty BC, Banthia AK. Poly(ethylene oxide)/clay nanocomposite: Thermomechanical properties and morphology. Polymer. 2006;47(11):4068-4074.
20. Azizi Samir MAS, Alloin F, Sanchez J-Y, Dufresne A. Cellulose nanocrystals reinforced poly(oxyethylene). Polymer. 2004;45(12):4149-4157.
21. Azizi Samir MAS, Chazeau L, Alloin F, Cavaillé JY, Dufresne A, Sanchez JY. POE-based nanocomposite polymer electrolytes reinforced with cellulose whiskers. Electrochim Acta. 2005;50(19):3897-3903.
22. Zhang H, Xia H, Zhao Y. Optically triggered and spatially controllable shape-memory polymer–gold nanoparticle composite materials. J Mater Chem. 2012;22(3):845-849.
23. Lu H, Liang F, Gou J, Leng J, Du S. Synergistic effect of Ag nanoparticle-decorated graphene oxide and carbon fiber on electrical actuation of polymeric shape memory nanocomposites. Smart Mater Struct. 2014;23(8):085034.
24. Telfah A, Abdul-Gader Jafar MM, Jum’h I, Ahmad MJA, Lambert J, Hergenröder R. Identification of relaxation processes in pure polyethylene oxide (PEO) films by the dielectric permittivity and electric modulus formalisms. Polym Adv Technol. 2018;29(7):1974-1987.
25. Mashtalyar DV, Imshinetskiy IM, Nadaraia KV, Gnedenkov AS, Sinebryukhov SL, Ustinov AY, et al. Influence of ZrO_2/SiO_2 nanomaterial incorporation on the properties of PEO layers on Mg-Mn-Ce alloy. Journal of Magnesium and Alloys. 2022;10(2):513-526.
26. Mohammed AJ, Al-nesrawy SH. Nano Ferrite Incorporated Poly (Vinyl Pyrrolidone (PVP) /Poly (Vinyl Alcohol (PVA) Blend: Preparation and Investigation of Structural, Morphological and Optical Properties. NeuroQuantology. 2022;20(4):251-258.
27. Al-Akhras MA, Alzoubi SE, Ahmad AA, Ababneh R, Telfah A. Studies of composite films of polyethylene oxide doped with potassium hexachloroplatinate. J Appl Polym Sci. 2020;138(5).
28. Hashim A, Agool IR, Kadhim KJ. Novel of (polymer blend-Fe_3O_4) magnetic nanocomposites: preparation and characterization for thermal energy storage and release, gamma ray shielding, antibacterial activity and humidity sensors applications. Journal of Materials Science: Materials in Electronics. 2018;29(12):10369-10394.
29. Abdullah OG, Saleem SA. Effect of Copper Sulfide Nanoparticles on the Optical and Electrical Behavior of Poly(vinyl alcohol) Films. J Electron Mater. 2016;45(11):5910-5920.
30. Fadil OB, Hashim A. Fabrication and Tailored Optical Characteristics of CeO_2/SiO_2 Nanostructures Doped PMMA for Electronics and Optics Fields. Silicon. 2022;14(15):9845-9852.
31. Rajesh K, Crasta V, Rithin Kumar NB, Shetty G, Rekha PD. Structural, optical, mechanical and dielectric properties of titanium dioxide doped PVA/PVP nanocomposite. Journal of Polymer Research. 2019;26(4).
32. Vashchuk A, Fainleib AM, Starostenko O, Grande D. Application of ionic liquids in thermosetting polymers: Epoxy and cyanate ester resins. Express Polymer Letters. 2018;12(10):898-917.
33. Obaid SF, Kadhim RG. The effect of Ag_2O/NbO_2 nanostructures on the dielectric characteristics of PVA/PVP bled used in electronics. Journal of Physics: Conference Series. 2022;2322(1):012080.
34. Mohammed BH, Sallehuddin H, Yadegaridehkordi E, Safie Mohd Satar N, Hussain AHB, Abdelghanymohamed S. Nexus between Building Information Modeling and Internet of Things in the Construction Industries. Applied Sciences. 2022;12(20):10629.
35. Zaman U, Imran, Mehmood F, Iqbal N, Kim J, Ibrahim M. Towards Secure and Intelligent Internet of Health Things: A Survey of Enabling Technologies and Applications. Electronics. 2022;11(12):1893.